SCIENTIFIC REPORTS
nature research

OPEN

64-Channel Carbon Fiber Electrode Arrays for Chronic Electrophysiology

Grigori Guitchounts[1,2,3*] & David Cox[1,2]

A chief goal in neuroscience is to understand how neuronal activity relates to behavior, perception, and cognition. However, monitoring neuronal activity over long periods of time is technically challenging, and limited, in part, by the invasive nature of recording tools. While electrodes allow for recording in freely-behaving animals, they tend to be bulky and stiff, causing damage to the tissue they are implanted in. One solution to this invasiveness problem may be probes that are small enough to fly under the immune system's radar. Carbon fiber (CF) electrodes are thinner and more flexible than typical metal or silicon electrodes, but the arrays described in previous reports had low channel counts and required time-consuming manual assembly. Here we report the design of an expanded-channel-count carbon fiber electrode array (CFEA) as well as a method for fast preparation of the recording sites using acid etching and electroplating with PEDOT-TFB, and demonstrate the ability of the 64-channel CFEA to record from rat visual cortex. We include designs for interfacing the system with micro-drives or flex-PCB cables for recording from multiple brain regions, as well as a facilitated method for coating CFs with the insulator Parylene-C. High-channel-count CFEAs may thus be an alternative to traditional microwire-based electrodes and a practical tool for exploring the neural code.

In order to understand information processing in the brain, scientists must be able to take reliable measurements from the central nervous system (CNS). Ideal methods would allow us to record from all neurons in a brain (10^8 in a rat or zebra finch[1] at cellular spatial resolution and a temporal resolution on which neurons operate (kHz range) in behaving animals[2,3]. While established methods for whole-brain monitoring (e.g. fMRI or PET) typically give poor spatial and temporal resolution, state of the art optical methods for imaging of genetically-encoded calcium indicators have yielded cellular spatial resolution while recording all neurons in a larval zebrafish brain (on the order of ~10^5 neurons) simultaneously at low temporal resolution (~0.5 Hz)[4,5], although faster dynamics are possible with optical methods, including with genetically-encoded voltage indicators or lightsheet microscopy[6,7].

In contrast to most imaging of calcium indicators, recording neuronal activity using electrodes provides spike-time temporal resolution but low cellular yield (state of the art simultaneously recorded neurons using Neuropixels probes is ~3000 neurons using 8 probes, each of which contains 384 recording sites, yielding roughly one unit per recording site[8,9]. A further limitation of electrode methods is their invasive nature: implanting large electrode arrays damages the tissue the electrodes are meant to record from[10,11], thus limiting the yield of recorded neurons, the longevity of the recording quality, and the ability to track the activity of individual neurons over long timescales. These are particularly pressing problems for investigations into how the neural code changes during learning, which unfolds over days, weeks or months[12–18]; or for the creation of practical brain-machine-interfaces (BMIs), which rely on the stability of recorded signals as well as the underlying neural code in order to decode a patient's thoughts or intended actions[13,19].

Metal electrodes have been used for recording single neurons since the mid-20th century[20]. These are typically tungsten or PtIR wires, on the order of 5–50 μm in diameter[21–23]. In rodent work, the typical approach involves arrays composed of individual metal wires spun into groups of four (tetrodes) and bundled into groups of up to 40 tetrodes, or 160 channels[24]. Monolithic silicon devices are a prominent alternative[8,25,26] that allows for high-density recording sites and high channel counts at the expense of a large cross-section (e.g. 70 × 20 μm in Neuropixels probes) and high stiffness, which make it a challenge to record on long-timescales (however, see Okun *et al.*[27]).

[1]Center for Brain Science, Harvard University, Cambridge, Massachusetts, 02138, USA. [2]Department of Molecular and Cellular Biology, Harvard University, Cambridge, MA, 02138, USA. [3]Program in Neuroscience, Harvard University, Cambridge, Massachusetts, 02138, USA. *email: guitchounts@fas.harvard.edu

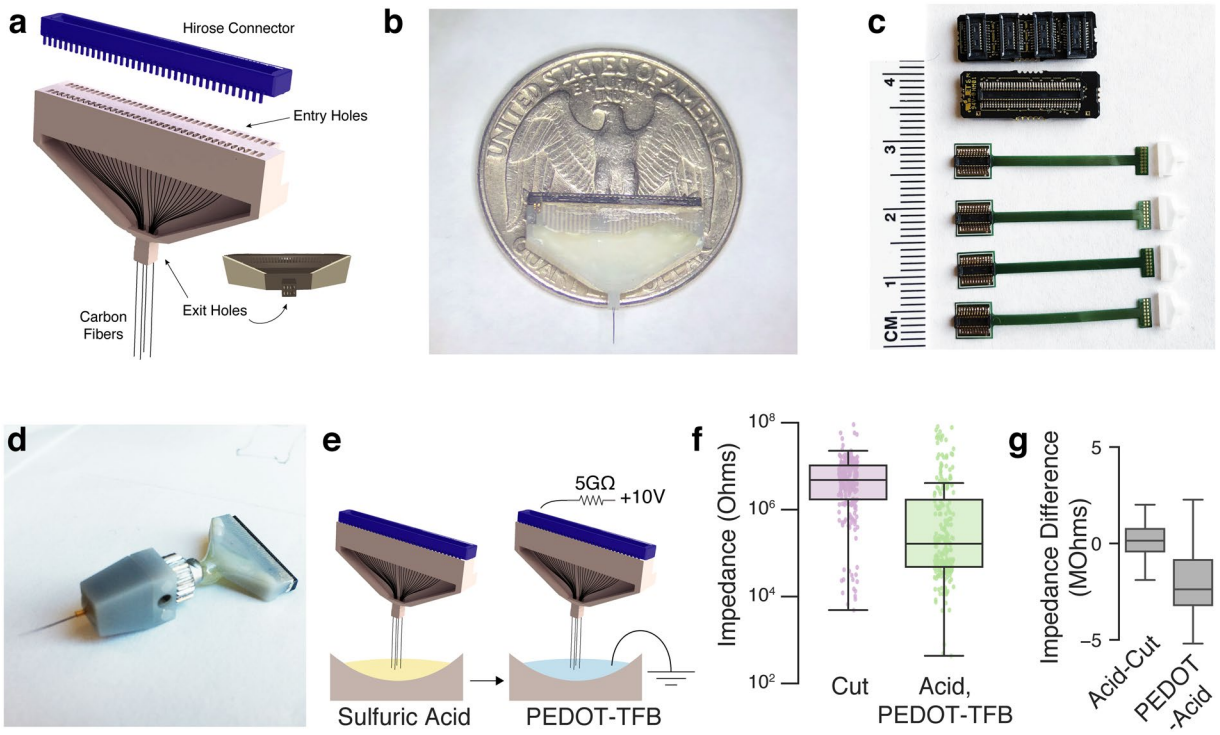

Figure 1. Assembly and Tip-Preparation. (**a**) Schematic of 64-channel 3D-printed block (grey) for holding carbon fibers (CFs). After threading the CFs through the block, the wells are filled with silver paint. A 70-pin Hirose connector (blue) mates with the wells. (**b**) Photo of assembled array with a US quarter. (**c**) System for multi-region recording using four 16-channel flex-PCB cables and 3D-printed blocks that mate with a PCB adapter for 64-channel recording (top). (**d**) A 64-channel CFEA mounted on a vented-screw micro-drive based on the design in Anikeeva *et al.*[35]. (**e**) The recording sites are prepared by dipping the CF tips into 99% sulfuric acid for 5 minutes (left). After washing any remaining acid off with water, the tips are electroplated with PEDOT-TFB by passing a 2nA current via a 10V source through a 5G-Ohm resistor for 1 minute per electrode. (**f**) Impedance of 224 wires across eight arrays (two 64-channel and six 16-channel) after cutting the tips with scissors (4.84 ± 0.68 MΩ, median ± s.e.m.) and after treatment with the acid and PEDOT-TFB (0.17 ± 0.86 MΩ). Each dot is one fiber. (**g**) Impedance change from the cut arrays after acid treatment (left; 0.14 ± 0.15, median ± S.E.M.) and from acid treatment to PEDOT-TFB plating (right; −2.38 ± 0.25, median ± S.E.M.).

Carbon fiber electrode arrays (CFEAs) are an alternative to metal wires or silicon probes. Carbon fibers are thinner and more flexible than metal wires typically used, and produce a lower immune response after being implanted into the CNS[10,28,29]. We have previously demonstrated a method for producing multi-channel carbon fiber arrays[30]. However, the previous design was low-channel-count and required time-consuming individual preparation of the recording sites (each electrode tip had to be fire-sharpened to reduce impedance).

Here we demonstrate the design of 64-channel CFEAs and a method for bulk preparation of the recording sites. The tips were prepared by etching with sulfuric acid in order to increase surface area[31,32], followed by electroplating with PEDOT-TFB[33,34], resulting in a dramatically decreased impedance. Recordings in rat visual cortex demonstrate the feasibility of recording neural signals with this method. Designs for the 64-channel array are freely available online (https://github.com/guitchounts/electrodes), as are designs for flex-PCB-based 16-channel arrays, which allow for recording from multiple brain areas simultaneously. Finally, we share designs for laser-cut cartridges that facilitate preparation of CFs for insulation with Parylene-C.

Results

Assembly and tip preparation. In this report, we tested two types of CF arrays: a 16-channel version (assembly of which was reported in[30], and an expanded 64-channel version. For the latter, we designed a 3D-printed plastic block to hold the 64 CFs (Fig. 1a). As in the 16-channel arrays, carbon fibers were threaded through wells at the top of the block, and down through the exit holes on the bottom. The pictured design features four exit holes, arranged in a 2×2 grid, but this arrangement can be modified to an 8 × 2 grid of exit holes (designs available at github.com/guitchounts/electrodes/) or a single exit hole to bundle the 64 CFs into one. In the implants described here, fibers were bundled into one set of 64. After threading, fibers protrude from the top wells and from the bottom exit holes. To connectorize the array, the top-well-protruding wires are first de-insulated (by a flame passed swiftly over the wires, to burn off the Parylene-C), then pushed farther into the wells until they no longer protrude through the top. Then, a dab of silver paint is applied to the wells (Fig. S1d); once it spreads through the wells, excess paint is brushed off with a cotton-tipped applicator (Fig. S1e,f), and a connector is placed into the wells (Fig. S1g,h). In the 64-channel version, this is a 70-pin Hirose connector whose pins were

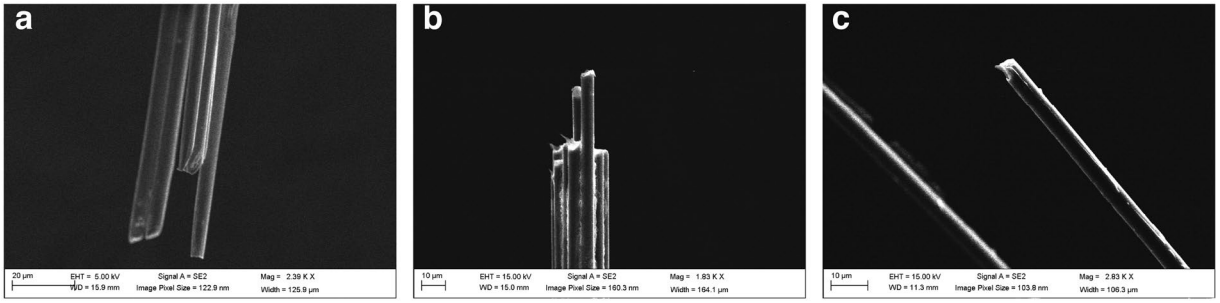

Figure 2. SEM Images of CF tips. (**a**) Several wires from a 16-channel array bundle before treatment. (**b**) Bundle after acid treatment. (**c**) Close-up of a single fiber after electroplating with PEDOT-TFB.

folded down manually before insertion (Figs. 1a; S1a–c). The connector is then glued to the plastic block with super glue. The design is configurable to single-block 64-channel arrays (Fig. 1b) or four 16-channel arrays on flex-cable PCBs for multi-brain-region recordings (Figs. 1c; S1i; S2), and is compatible with micro-drive devices (Fig. 1d)[35].

The impedance of untreated tips is too high for single-unit recordings in a fixed-implant preparation[36], requiring treatment before recordings can be made. In a previous report, tips were prepared by individual fire-sharpening, which de-insulated ~80 μm along the shaft of each wire, simultaneously sharpening it[30]. While successful, this technique is difficult to scale to high-channel-count arrays. To get around this problem, we turned to chemical treatment of the tips, first etching the tips using sulfuric acid in order to roughen the tip surface and increase the surface area[31,32], then electroplating the tips with PEDOT-TFB, which was previously shown to reduce impedance and increase conductivity and stability compared to the more conventionally used PEDOT-PSS[33,34] (Fig. 1e). The resulting tips had significantly reduced impedances (before treatment: 4.84 ± 0.68 MΩ median ± s.e.m. ($n = 224$ tips from two 64-channel and six 16-channel arrays), and 0.17 ± 0.86 MΩ in the same tips after treatment with the acid and PEDOT-TFB (two-sided t-test on impedance before/after treatment of tips: $t = 3.88$, $p = 0.00014$)) (Fig. 1f). The bulk of the impedance change following the acid and PEDOT-TFB treatments came from the electroplating rather than etching (Fig. 1g). Following acid etching and electroplating with PEDOT-TFB, ~15% of tips retained an impedance of at least 4.84 MΩ (the pre-treatment median), which likely include dead channels. We visualized the effect of this treatment on the tips using scanning electron microscopy on 16-channel arrays (Fig. 2).

The CFEA requires individual carbon fibers to be insulated with parylene-C before assembly, which in our previous design involved a painstaking manual procedure in which individual fibers were mounted on sticky notes and loaded into the parylene vapor deposition machine (PDS Labcoter 2010). To facilitate this process, we designed coating jigs (Fig. 3a–c) that hold multiple cartridges (Fig. 3d,e), each of which in turn hold several dozen carbon fibers splayed harp-like across two pieces of sticky notes. This design (Fig. 3f) can be laser-cut out of plastic and modified to various sizes of cartridges (to hold longer fibers, for example) or jigs (to hold more or fewer cartridges).

Long-term recordings. We tested the longevity of acid/PEDOT-TFB-treated arrays by recording chronically from a 16-channel version of the array implanted in rat primary visual cortex (V1). Figure 4 shows examples from one such implanted rat. Fig. 4a shows two seconds of bandpass-filtered activity four days after the implant surgery ('Day 4'), while Fig. 4b shows activity from the same array 55 days later. Spiking activity was prominent across most channels in both recordings. We performed spike sorting on both recording sessions using automated clustering based on the ISO-SPLIT algorithm (MountainSort[37]), and found a minor decrease in signal to noise ratios of well-isolated sorted units (2.90 ± 0.36 (mean ± s.e.m.) on day 4 post surgery, and 2.38 ± 0.43 55 days later ($t = 0.70$, $p = 0.49$, t-test)), virtually unchanged isolation metric (0.99 ± 0.01 (mean ± s.e.m.) on day 4 post surgery, and 0.98 ± 0.02 55 days later ($t = 0.64$, $p = 0.53$, t-test)), and a somewhat increased noise metric (0.19 ± 0.03 (mean ± s.e.m.) on day 4 post surgery, and 0.23 ± 0.06 55 days later ($t = -0.76$, $p = 0.46$, t-test)). We repeated the spike sorting on two more recording sessions from another rat, for a total of $n = 37$ isolated units across the four sessions in two rats (Fig. 4d).

64-Channel recording and responses to visual stimulation. We then proceeded to implant the 64-channel arrays into rat V1. Figure 5 shows example traces from one such recording while the animal was behaving freely in the recording chamber. Having determined that we could record spontaneous neuronal activity using chronically-implanted 64-channel CF arrays, we sought to determine whether these arrays could capture sensory evoked activity as well. For this, we presented a V1-implanted rat with a visual stimulus: flashed cage lights. The rat was free to behave in the recording chamber in the dark, while the cage lights were flashed (On for 500 milliseconds, Off for a uniformly random time between 400 and 600 milliseconds, for 225 trials.). This strong visual stimulus produced evoked multiunit (MU) responses (Fig. 6a,b) and LFPs (Fig. 6c). Figure 6a shows one trial (grey patch indicates time when lights were On); Figure 6b,c show trial-averaged MU and LFP responses, respectively. The mean LFP response showed a strong modulation following stimulus onset, as well as a smaller response following stimulus offset, as has previously been reported[38–40].

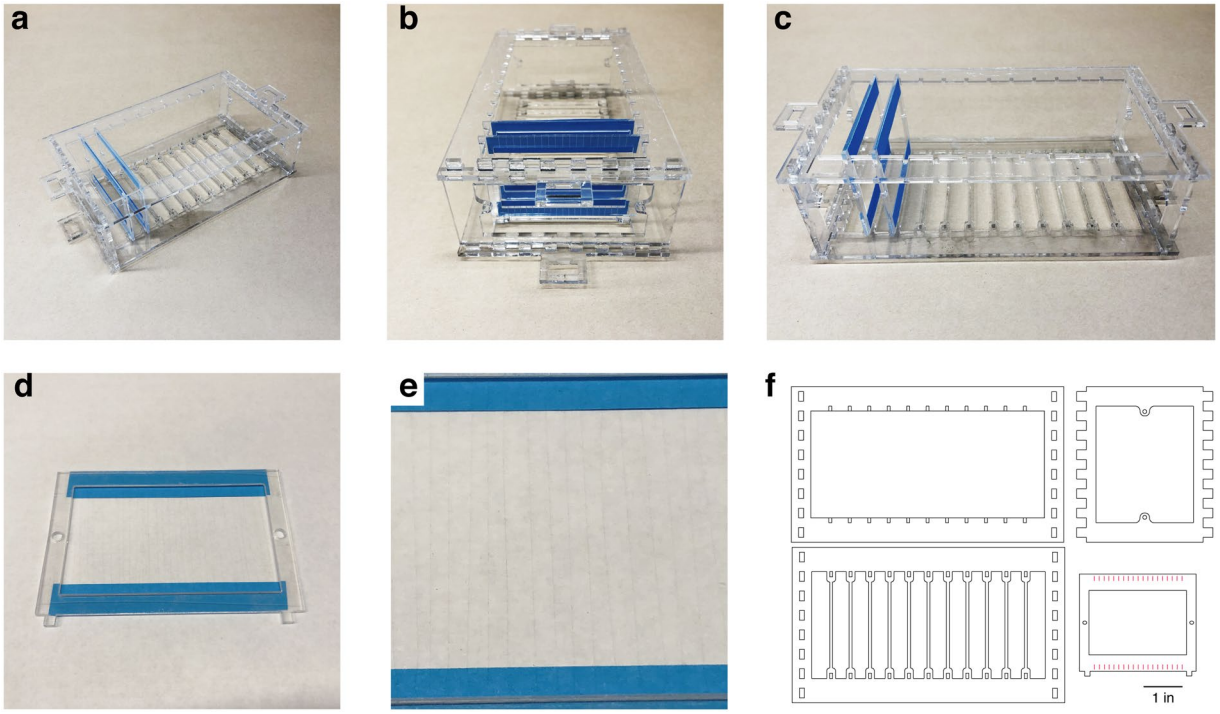

Figure 3. Parylene Coating Jig. (**a–c**) The assembled jig with two CF cartridges. (**d**) An example cartridge. Each cartridge holds 20–30 CFs, which are strung out across two sticky notes attached to the cartridge. (**e**) The fibers are placed across the cartridge like strings on a harp. (**f**) Jig and cartridge designs. Each jig holds 11 cartridges, but this design may be expanded as long as the jig fits into the Parylene deposition machine (PDS Labcoter 2010).

Finally, to test for potential cross-talk among channels in the CFEA, we measured correlations among pairs of bandpass-filtered 30-second traces and compared these pairwise correlations to data obtained from recordings using nichrome wire tetrodes implanted in rat V1 (Fig. S3). The nichrome tetrode arrays were arranged in an 8×2 grid, with ~300-micron spacing among tetrodes. This spacing allowed us to compare correlations among pairs of carbon fibers to those of closely spaced nichrome wires (i.e. within a given tetrode) and distant nichrome wires (i.e. across tetrodes). We reasoned that making these comparisons would provide a better understanding of the degree of cross-talk within the closely-spaced carbon fibers. Correlations among channels in the CFEA were comparable to, albeit slightly lower than, those within nichrome tetrodes, consistent with the idea that the devices presented here are capable of recording independent neural signals despite the close bundling of the fibers.

Discussion

CFEAs have shown promise in recording from neuronal populations over long timescales but have so far been prepared in small channel-count configurations[28,30,41–43]. It is becoming increasingly clear that in order to understand the brain, neuroscientists will need to measure larger populations of neurons spread out across multiple brain regions[8] (however, see Gao *et al.*[44]). Our results show the feasibility of producing high channel-count, high-density CFEAs and using them to record evoked activity in rat visual cortex. Further, we have shared designs to implement simultaneous recordings from multiple brain regions using four 16-channel flex-PCB CFEAs (Fig. 1c) and micro-drive-enabled 64-channel arrays (Fig. 1d). We have also designed a jig for setting up Parylene-C deposition onto the bare CFs (Fig. 3), which we hope will facilitate the implementation of CFEAs by other labs.

The 64-channel CFEAs are faster to assemble (per channel) than their 16-channel predecessors (~2 hours for the former and ~1 hour for the latter: a 2X improvement from 3.75 to 1.875 minutes/channel). Although etching and electroplating with PEDOT-TFB are not by themselves new techniques, neither has previously been applied to CFEAs. The method of preparing the recording sites using acid etching and electroplating with PEDOT-TFB further sped up the assembly process over the previous fire-sharpening technique, which was done on individual fibers and required extensive practice[30].

CFEA designs have for the most part required manual assembly. This will obviously make recording extremely large populations of neurons (10^{5-6}) a challenge. As such, manually-assembled CFEAs may be a more appropriate alternative to other manually-made electrodes like tetrodes, rather than arrays manufactured using nanotechnology[8,25,26], which may soon be able to accommodate thousands of recording sites. CFEAs are smaller and more flexible than many silicon probes, although still stiffer than brain tissue; efforts to further reduce the stiffness of electrodes are proving to be a successful strategy for improving recording technology[45]. Previous reports have shown CFEAs to produce a smaller immune response than larger implants[11,42,46], and further experiments will be

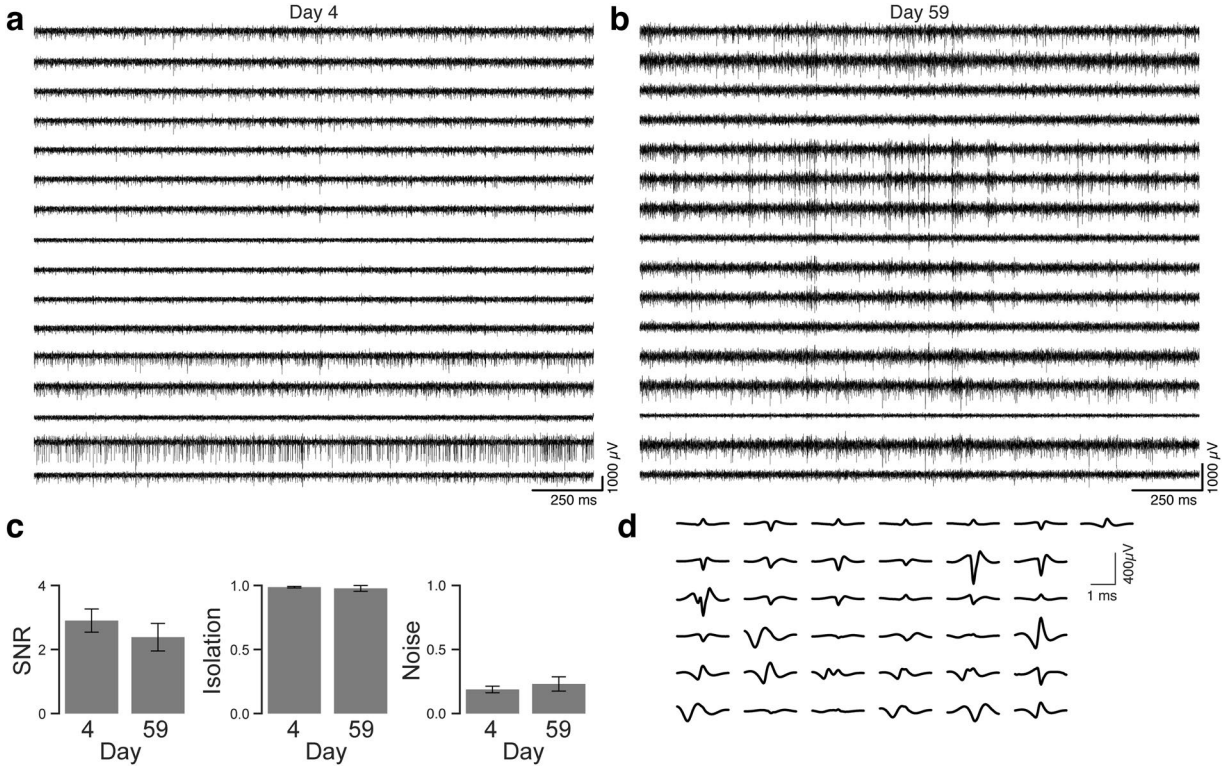

Figure 4. Chronic Recordings. Example of 2 seconds of filtered activity traces from a 16-channel CF array chronically implanted in rat visual cortex, with activity sampled four days after implant surgery **(a)** and recording from the same animal 55 days later **(b)**. **(c)** Properties of sorted single units across the two recording sessions in (**a**,**b**), with signal to noise ratio (SNR), isolation, and noise. **(d)** Mean waveforms of sorted units across four recording sessions in two rats.

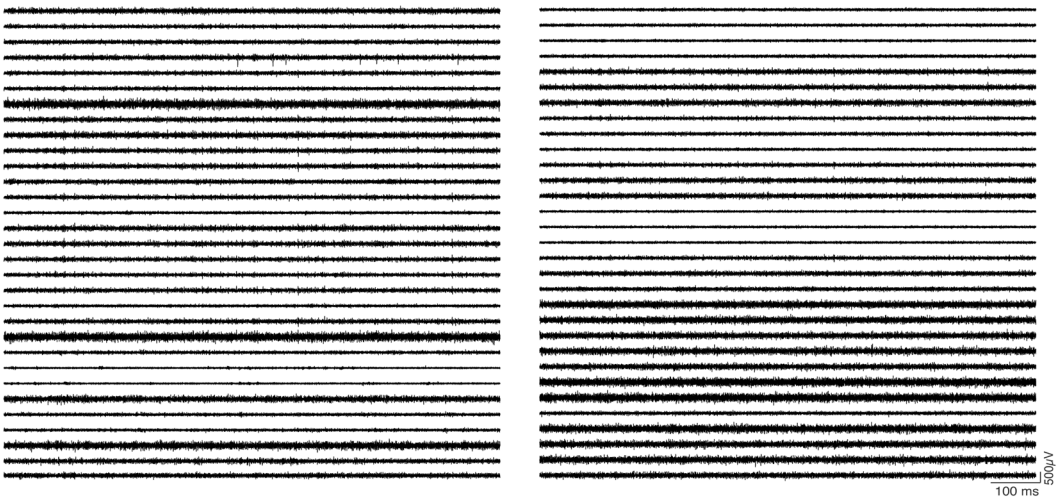

Figure 5. Example traces from 64-channel array. One second of raw filtered activity recorded from one 64-channel CF array implanted in rat V1 showing multiunit signals. Left column: first half of the channels; right column: the remaining channels. Two dead channels have been removed from the graph.

required to assess the immune responses of large channel-count arrays such as those described here. While manual assembly of CFEAs limits their scalability, they can, in principle, be manufactured using automated systems, and some efforts are underway to implement those[47].

Electrode arrays are currently the best tool for investigating neuronal circuits continuously (i.e. 24/7) over long periods of time in freely behaving animals. However, whether electrode arrays of any kind will be the method to record all the neuronal activity in a brain is still unknown. Arrays designed to capture the entirety of neuronal

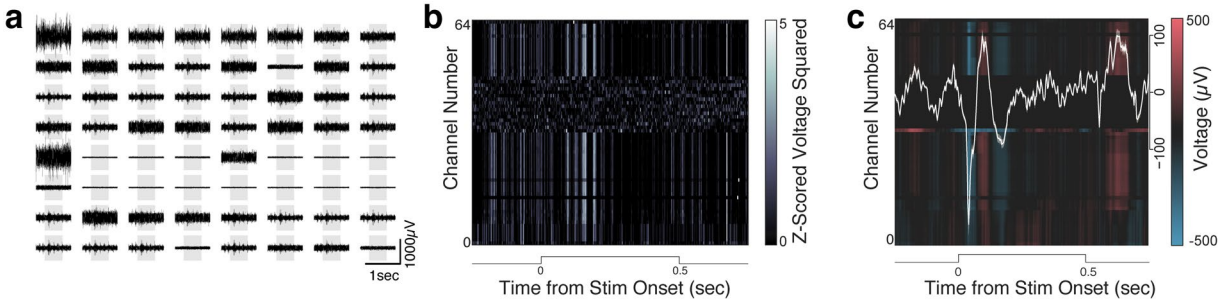

Figure 6. Visual Cortex Responses to Visual Stimulation. The stimulus was a 500-millisecond light flash delivered while the rat moved freely in the recording chamber. (**a**) Filtered raw traces across 64 CF electrodes during one stimulation trial (grey patch symbolizes the duration of the light flash) showing multiunit (MU) responses to the stimulus. (**b**) Mean MU response across 225 trials of the light flash (filtered traces were z-scored, squared, and smoothed with a gaussian filter). (**c**) Mean LFP (300 Hz low-pass filtered) response across the same trials (white line: mean LFP response across channels). A handful of channels (#34–36, 38–40, 42–48) in this example were nonfunctional.

activity in a vertebrate brain would need to be quite noninvasive indeed; they would also need to capture the activity of millions of neurons, which would require multiplexing and digitization near the recording sites[48].

Alternatives to electrodes might be optical methods, which are currently limited in their ability to image deep brain structures[49]. Imaging of calcium indicators has a limited temporal resolution because of molecular binding kinetics[50]. This problem may be avoided by voltage sensors, which can be imaged at kilohertz rates[6,51,52], but in principle suffer from the same depth imaging and bleaching problems as calcium indicators[53]. One radically different approach is molecular barcoding, in which neuronal activity is recorded by a 'molecular ticker-tape' that tracks changes in intracellular calcium concentration by making insertions into a cell's DNA[54,55]. For now, perhaps the best way to get around the limitations of each technique is to use multiple complementary tools, investigating local circuits with electrode arrays after a brain region of interest is identified using whole-brain low-temporal-resolution methods like calcium imaging or fMRI.

Methods

Animals. All procedures were performed in accordance with institutional guidelines and regulations. The care and experimental manipulation of all animals were reviewed and approved by the Harvard Institutional Animal Care and Use Committee (Protocol #27-22). Experimental subjects were female Long Evans rats 3 months or older, weighing 300–500 grams ($n = 6$, Charles River). Two rats were implanted with 16-channel arrays; two were implanted with 64-channel arrays; one was implanted with four 16-channel arrays in different brain regions; and one was implanted with a 16-tetrode nichrome wire array in visual cortex.

Carbon fibers, array assembly, and tip preparation. In this report, we used 4.5μm diameter carbon fibers (UMS2526, Goodfellow USA), as reported previously[30]. Epoxy sizing was removed either by heating the fibers to 400 C in a kiln, or by soaking the fibers in acetone >24 hours[56]. To insulate the fibers with Parylene-C (di-chloro-di-p-xylylene) (Paratronix Inc, Westborough MA), we laid the fibers out onto sticky notes attached to plastic cartridges (Fig. 3) and coated the fibers with ~1μm layer of Parylene-C using chemical vapor deposition in a PDS-2010 Labcoter machine (Specialty Coating Systems, http://scscoatings.com/), as described previously[30].

The fibers were then threaded through 3D-printed plastic blocks, which were custom-designed in SolidWorks (Dassault Systémes SolidWorks Corporation, Waltham, MA) and manufactured using stereolithography (Realize Inc, Noblesville, IN) (designs available on https://github.com/guitchounts/electrodes). The fibers were left protruding ~1 mm from the top of the plastic block (i.e. at the entry holes) end and were then deinsulated at the connectorization end with a lighter flame, after which they were threaded further into the block until no longer protruding. Connectorization was achieved by flooding the block's wells with silver paint (MG Chemicals, #842-20g) and attaching a Hirose DF40 connector (Digi-key, H11630CT-ND).

The recording sites were prepared by cutting the array bundles to the desired length for implantation (~1 mm for the visual cortex implants described here) using serrated scissors (Fine Science Tools, 14058-11), then dipping the tips into 99% sulfuric acid (Sigma, 339741–500 ML) for 5 minutes, then (after washing any remaining acid off with water), and electroplating with PEDOT-TFB[33,34] by applying a 2 nA current via a 10 V power supply in series with a 5000 MΩ resistor (Digikey, SM102035007FE-ND), for 1 minute (for a total charge delivery of 120nC) per electrode[28]. The electroplating solution consisted of 0.01 M EDOT (Sigma, 483028-10G) and 0.1 M tetrabutylammonium tetrafluoroborate (TFB) (Sigma, 86896–25 G) in acetonitrile (Sigma, 360457–500 ML). The impedance was tested at 1 kHz using an Intan-based headstage and OpenEphys GUI (http://www.open-ephys.org/gui/).

Surgery. Animals were anesthetized with 2% isoflurane and placed into a stereotaxic apparatus (Knopf Instruments). Care was taken to clean the scalp with Povidone-iodine swabsticks (Professional Disposables International, #S41125) and isopropyl alcohol (Dynarex #1204) before removing the scalp and cleaning the skull surface with hydrogen peroxide (Swan) and a mixture of citric acid (10%) and ferric chloride (3%) (Parkell #S393).

Three skull screws (Fine Science Tools, #19010-00) were screwed into the skull to anchor the implant. A 0.003″ stainless steel (A-M Systems, #794700) ground wire was inserted ~2 mm tangential to the brain over the cerebellum.

The arrays were targeted to right V1, ranging ~6–8 mm posterior to bregma, 4.5 mm ML, reaching layer 2/3 at 0.6 mm DV. After electrodes were inserted into the brain, the craniotomy was covered with Puralube vet ointment (Dechra) and the electrodes were glued down with Metabond (Parkell). Post-operative care included twice-daily injections of buprenex (0.05 mg/kg Intraperitoneal (IP)) and dexamethasone (0.5 mg/kg IP) for three days.

Electrophysiology. Electrode signals were acquired at 30 kHz using either a 16-channel Intan RHD2132 headstage, or a custom Intan-based 64-channel headstage[57] and Opal-Kelly FPGAs (XEM6010 with Xilinx Spartan-6 ICs). LFPs and spikes were extracted following procedures described in Dhawale *et al.*[57]. The LFP signals were downsampled to 300 Hz by two applications of a fourth order 5-fold decimating Chebychev filter followed by a single application of a fourth order 4-fold decimating Chebychev filter. The 16-channel data were acquired using the OpenEphys GUI[58]. Units presented in Figure 4 were sorted using the MountainSort package[37].

In addition to the 64-channel CFEAs, we designed a 64-channel system for recording with four 16-channel arrays in multiple brain regions. The 16-channel flex-PCB (Fig. 1c) mates with a miniature 16-channel 3D-printed plastic block that holds the CFs. The connector side holds a 20-pin Hirose DF40 connector (Digi-key, H11618CT-ND) that interfaces with a breakout PCB that holds four mating 20-pin connectors (Digi-key, H11619CT-ND) on one side and a 70-pin DF40 connector (Digi-key, H11630CT-ND) on the other. The breakout board thus connects four flex-PCB arrays to one 64-channel headstage. The four flex-PCB arrays could be mounted on microdrives as in Vandecasteele *et al.*[59]. The 64-channel CFEAs were also adapted for microdrive-based recordings based on the optetrode design in Anikeeva *et al.*[35]. In our design, the 64-channel array and microdrive are assembled separately and joined using micromanipulators. Specifically, the carbon fibers in the assembled array are bundled together, then threaded through a polyimide tube attached to the microdrive. The plastic base of the array is then glued to the vented screw in which the polyimide tube and carbon fibers reside (Fig. 1d). In this design, the entire 64-channel bundle is driven as one unit, in contrast to tetrode-based microdrives that allow for advancing of individual tetrodes[60].

To compare the cross-talk and correlation structure of signals recorded from CFEA to those from traditional nichrome wire tetrode arrays (Fig. S3), we implanted one rat with a 16-tetrode nichrome array in V1. Tetrodes were fabricated using 12.5-micron nichrome wire (Sandvik-Kanthal) following standard procedures[58,61,62]. Tetrodes were threaded through 42 AWG polyimide guide tubes into 8x2 grids of 34 AWG tubes (Small Parts). The tetrodes were plated with a mixture of gold (Neuralynx) and polyethylene glycol (PEG) as per Ferguson *et al.*[63], to an impedance of ~100–250 KΩ. The ground and reference wires were bridged and implanted through a craniotomy above the cerebellum.

Behavior and visual stimulation. The recordings were carried out in a custom recording chamber while the animals were free to behave. The headstage was connected to the FPGA board via a custom shielded cable (Samtec, SFSD-07-30C-H-12.00-DR-NDS, TFM-107-02-L-D-WT; McMaster extension spring 9640K123) and commutator (Logisaf 22 mm 300 Rpm 24 Circuits Capsule Slip Ring 2A 240 V Test Equipment, Amazon).

Visual stimulation was delivered via white LED lights (Triangle Bulbs Cool White LED Waterproof Flexible Strip Light, T93007-1, Amazon) mounted in the recording chamber, and controlled with a micro-controller (Arduino). During stimulus presentation, the chamber and experimental room were otherwise completely dark. The lights were On for 500 ms and Off for a uniform-random time between 400 and 600 ms.

Imaging. Scanning Electron Microscopy images of the CF tips were taken using a Zeiss Ultra55 Field Emission Scanning Electron Microscope (FESEM) at the Center for Nanoscale Systems at Harvard University.

Received: 11 July 2019; Accepted: 17 February 2020;
Published online: 02 March 2020

References

1. Olkowicz, S. *et al*. Birds have primate-like numbers of neurons in the forebrain. *PNAS* **113**, 201517131–7260 (2016).
2. Alivisatos, A. P. *et al*. Nanotools for Neuroscience and Brain Activity Mapping. *ACS Nano* **7**, 1850–1866 (2013).
3. Buzsáki, G., Anastassiou, C. A. & Koch, C. The origin of extracellular fields and currents-eeg, ecog, lfp and spikes. *Nature Reviews Neuroscience* **13**, 407 (2012).
4. Dunn, T. W. *et al*. Brain-wide mapping of neural activity controlling zebrafish exploratory locomotion. *eLife* **5**, e12741 (2016).
5. Vladimirov, N. *et al*. Light-sheet functional imaging in fictively behaving zebrafish. *Nature Methods* **11**, 883–884 (2014).
6. Villette, V. *et al*. Ultrafast two-photon imaging of a high-gain voltage indicator in awake behaving mice. *Cell* **179**, 1590–1608 (2019).
7. Hillman, E. M., Voleti, V., Li, W. & Yu, H. Light-sheet microscopy in neuroscience. *Annual review of neuroscience* **42**, 295–313 (2019).
8. Jun, J. J. *et al*. Fully integrated silicon probes for high-density recording of neural activity. *Nature* **551**, 232–236 (2017).
9. Stringer, C. *et al*. Spontaneous behaviors drive multidimensional, brainwide activity. *Science* **364**, 255 (2019).
10. Biran, R., Martin, D. C. & Tresco, P. A. Neuronal cell loss accompanies the brain tissue response to chronically implanted silicon microelectrode arrays. *Experimental neurology* **195**, 115–126 (2005).
11. Kozai, T. D. Y., Jaquins-Gerstl, A. S., Vazquez, A. L., Michael, A. C. & Cui, X. T. Brain Tissue Responses to Neural Implants Impact Signal Sensitivity and Intervention Strategies. *ACS Chemical Neuroscience* **6**, 48–67 (2014).
12. Kawai, R. *et al*. Motor Cortex Is Required for Learning but Not for Executing a Motor Skill. *Neuron* **86**, 800–812 (2015).
13. Koralek, A. C., Jin, X., Long, J. D. II, Costa, R. M. & Carmena, J. M. Corticostriatal plasticity is necessary for learning intentional neuroprosthetic skills. *Nature* **483**, 331–335 (2012).
14. Mooney, R. Neurobiology of song learning. *Current Opinion in Neurobiology* **19**, 654–660 (2009).
15. Poort, J. *et al*. Learning Enhances Sensory and Multiple Non-sensory Representations in Primary Visual Cortex. *Neuron* **86**, 1478–1490 (2015).
16. Ramanathan, D. S., Gulati, T. & Ganguly, K. Sleep-Dependent Reactivation of Ensembles in Motor Cortex Promotes Skill Consolidation. *PLoS Biology* **13**, e1002263 (2015).

17. Veit, L., Pidpruzhnykova, G. & Nieder, A. Associative learning rapidly establishes neuronal representations of upcoming behavioral choices in crows. *PNAS* **112**, 15208–15213 (2015).
18. Zoccolan, D., Oertelt, N., DiCarlo, J. J. & Cox, D. D. A rodent model for the study of invariant visual object recognition. *PNAS* **106**, 8748–8753 (2009).
19. Lebedev, M. A. & Nicolelis, M. A. L. Brain-Machine Interfaces: From Basic Science to Neuroprostheses and Neurorehabilitation. *Physiological Reviews* **97**, 767–837 (2017).
20. Hubel, D. H. Tungsten microelectrode for recording from single units. *Science* **125**, 549–550 (1957).
21. Gray, C. M., Maldonado, P. E., Wilson, M. & McNaughton, B. Tetrodes markedly improve the reliability and yield of multiple single-unit isolation from multi-unit recordings in cat striate cortex. *Journal of Neuroscience Methods* **63**, 43–54 (1995).
22. Lehew, G. & Nicolelis, M. A. L. *State-of-the-Art Microwire Array Design for Chronic Neural Recordings in Behaving Animals*. Frontiers in Neuroscience (CRC Press, Boca Raton (FL), 2008), 2nd edn.
23. Obaid, A. M. *et al*. Massively parallel microwire arrays integrated with cmos chips for neural recording. *bioRxiv* 573295 (2019).
24. Pfeiffer, B. E. & Foster, D. J. Hippocampal place-cell sequences depict future paths to remembered goals. *Nature* **497**, 74 (2013).
25. Kipke, D. R. *et al*. Advanced neurotechnologies for chronic neural interfaces: new horizons and clinical opportunities. *Journal of Neuroscience* **28**, 11830–11838 (2008).
26. Scholvin, J. *et al*. Close-Packed Silicon Microelectrodes for Scalable Spatially Oversampled Neural Recording. *IEEE Transactions on Biomedical Engineering* **63**, 120–130 (2015).
27. Okun, M., Lak, A., Carandini, M. & Harris, K. D. Long Term Recordings with Immobile Silicon Probes in the Mouse Cortex. *PLoS ONE* **11**, e0151180 (2016).
28. Kozai, T. D. Y. *et al*. Ultrasmall implantable composite microelectrodes with bioactive surfaces for chronic neural interfaces. *Nature Materials* **11**, 1065 (2012).
29. Polikov, V. S., Tresco, P. A. & Reichert, W. M. Response of brain tissue to chronically implanted neural electrodes. *Journal of Neuroscience Methods* **148**, 1–18 (2005).
30. Guitchounts, G., Markowitz, J. E., Liberti, W. A. & Gardner, T. J. A carbon-fiber electrode array for long-term neural recording. *Journal of Neural Engineering* **10**, 046016 (2013).
31. Tiwari, S. & Bijwe, J. Surface Treatment of Carbon Fibers - A Review. *Procedia Technology* **14**, 505–512 (2014).
32. Nohara, L. B., Petraconi Filho, G., Nohara, E. L., Kleinke, M. U. & Rezende, M. C. Evaluation of carbon fiber surface treated by chemical and cold plasma processes. *Materials Research* **8**, 281–286 (2005).
33. Charkhkar, H. *et al*. Chronic intracortical neural recordings using microelectrode arrays coated with PEDOT-TFB. *Acta Biomaterialia* **32**, 1–11 (2015).
34. Mandal, H. S. *et al*. Improving the performance of poly(3,4-ethylenedioxythiophene) (PEDOT) for brain machine interface applications. *Acta Biomaterialia* 1–31 (2014).
35. Anikeeva, P. *et al*. Optetrode: a multichannel readout for optogenetic control in freely moving mice. *Nature Neuroscience* **15**, 163–170 (2012).
36. Hill, D. N., Mehta, S. B. & Kleinfeld, D. Quality Metrics to Accompany Spike Sorting of Extracellular Signals. *Journal of Neuroscience* **31**, 8699–8705 (2011).
37. Chung, J. E. *et al*. A fully automated approach to spike sorting. *Neuron* **95**, 1381–1394 (2017).
38. Gavornik, J. P. & Bear, M. F. Learned spatiotemporal sequence recognition and prediction in primary visual cortex. *Nature Neuroscience* **17**, 732–737 (2014).
39. Hengen, K. B., Lambo, M. E., Van Hooser, S. D., Katz, D. B. & Turrigiano, G. G. Firing rate homeostasis in visual cortex of freely behaving rodents. *Neuron* **80**, 335–342 (2013).
40. Toda, H. *et al*. Simultaneous recording of ECoG and intracortical neuronal activity using a flexible multichannel electrode-mesh in visual cortex. *NeuroImage* **54**, 203–212 (2011).
41. Massey, T. L. *et al*. A high-density carbon fiber neural recording array technology. *Journal of Neural Engineering* **16**, 016024 (2019).
42. Patel, P. R. *et al*. Chronic in vivo stability assessment of carbon fiber microelectrode arrays. *Journal of Neural Engineering* **13**, 1–15 (2016).
43. Gillis, W. F. *et al*. Carbon fiber on polyimide ultra-microelectrodes. *Journal of Neural Engineering* **15**, 016010 (2018).
44. Gao, P. *et al*. A theory of multineuronal dimensionality, dynamics and measurement. *biorXiv* 1–50 (2017).
45. Hong, G., Yang, X., Zhou, T. & Lieber, C. M. Mesh electronics: a new paradigm for tissue-like brain probes. *Current opinion in neurobiology* **50**, 33–41 (2018).
46. Kozai, T. D. Y. *et al*. Effects of caspase-1 knockout on chronic neural recording quality and longevity: Insight into cellular and molecular mechanisms of the reactive tissue response. *Biomaterials* **35**, 9620–9634 (2014).
47. Massey, T. L. *et al*. Open-source automated system for assembling a high-density microwire neural recording array. *2016 International Conference on Manipulation, Automation and Robotics at Small Scales (MARSS)* 1–7 (2016).
48. Angotzi, G. N. *et al*. SiNAPS: An implantable active pixel sensor CMOS-probe for simultaneous large-scale neural recordings. *Biosensors and Bioelectronic* **126**, 355–364 (2019).
49. Yang, W. & Yuste, R. In vivo imaging of neural activity. *Nature Methods* **14**, 349–359 (2017).
50. Lin, M. Z. & Schnitzer, M. J. Genetically encoded indicators of neuronal activity. *Nature Neuroscience* **19**, 1142–1153 (2016).
51. Piatkevich, K. D. *et al*. A robotic multidimensional directed evolution approach applied to fluorescent voltage reporters. *Nature Chemical Biology* **14**, 1–17 (2018).
52. Adam, Y. *et al*. Voltage imaging and optogenetics reveal behaviour-dependent changes in hippocampal dynamics. *Nature* 1–26 (2019).
53. Platisa, J. & Pieribone, V. A. Genetically encoded fluorescent voltage indicators: are we there yet? *Current Opinion in Neurobiology* **50**, 146–153 (2018).
54. Glaser, J. I. *et al*. Statistical Analysis of Molecular Signal Recording. *PLoS Computational Biology* **9**, e1003145–14 (2013).
55. Kebschull, J. M. & Zador, A. M. Cellular barcoding: lineage tracing, screening and beyond. *Nature Methods* **15**, 1–9 (2018).
56. Wu, Q. *et al*. Effect of sizing on the interfacial properties of carbon fiber/bmi under different processing temperature. In *The 19th international conference on composite materials* (2013).
57. Dhawale, A. K. *et al*. Automated long-term recording and analysis of neural activity in behaving animals. *eLife* **6**, 91 (2017).
58. Siegle, J. H. *et al*. Open Ephys: an open-source, plugin-based platform for multichannel electrophysiology. *Journal of Neural Engineering* **14**, 045003–14 (2017).
59. Vandecasteele, M. *et al*. Large-scale recording of neurons by movable silicon probes in behaving rodents. *JoVE (Journal of Visualized Experiments)* e3568 (2012).
60. Voigts, J., Siegle, J. H., Pritchett, D. L. & Moore, C. I. The flexdrive: an ultra-light implant for optical control and highly parallel chronic recording of neuronal ensembles in freely moving mice. *Frontiers in systems neuroscience* **7**, 8 (2013).
61. Nguyen, D. P. *et al*. Micro-drive array for chronic *in vivo* recording: tetrode assembly. *JoVE (Journal of Visualized Experiments)* (2009).
62. Kloosterman, F. & Davidson, T. J. Journal of, S. G. J. & 2009. Micro-drive array for chronic *in vivo* recording: drive fabrication. *jove.com* (2009).
63. Ferguson, J. E., Boldt, C. & Redish, A. D. Creating low-impedance tetrodes by electroplating with additives. *Sensors and actuators. A, Physical* **156**, 388–393 (2009).

Acknowledgements
We would like to thank Andrea Stacy for assistance with SEM imaging at the Center for Nanoscale Systems at Harvard and Guosong Hong for advice on acid etching. We are immensely grateful to Jeffrey Markowitz, Steffen Wolff, Robert Johnson, and Javier Masis for comments on the manuscript. G.G. was supported by the National Science Foundation (NSF) Graduate Research Fellowship Program (GRFP).

Author contributions
G.G. conceived and performed the experiments, analyzed the data, and wrote the manuscript. D.C. provided research funding.

Competing interests
G.G. is named as an inventor on US patent no. US20170007824A1 filed by Boston University.

Additional information
Supplementary information is available for this paper at https://doi.org/10.1038/s41598-020-60873-y.

Correspondence and requests for materials should be addressed to G.G.

Reprints and permissions information is available at www.nature.com/reprints.

Publisher's note Springer Nature remains neutral with regard to jurisdictional claims in published maps and institutional affiliations.